Lidar for Aerosol Remote Sensing

27

Matthias Wiegner

Abstract

Measurements of aerosols are urgently required for understanding and modeling their role in the climate system and for investigating interactions between aerosols, clouds and radiation. Lidar (light detection and ranging) is an active remote sensing method for aerosol analysis which provides range resolved information. In this paper the different aerosol properties—geometrical, optical and microphysical—that can be derived from lidars are briefly described. In particular, the role of the so-called lidar ratio is discussed.

27.1 Introduction

Atmospheric aerosols not only influence the radiation budget, air chemistry and the hydrological cycle, but can also have an adverse influence on human health and the environment. Due to the large variety of aerosol sources and sinks and complex modification processes during their lifetime it is obvious that the optical and microphysical properties of the aerosols and their vertical layering may change in time and space. As a consequence, monitoring their distribution and characterizing their properties is a challenging task requiring advanced observation techniques. In particular, it is necessary to have a measuring system that can provided range resolved information.

M. Wiegner (✉)
Ludwig-Maximilians-Universität München (LMU), Meteorological Institute Munich (MIM), Theresienstraße 37, 80333 München, Germany
e-mail: m.wiegner@lmu.de

U. Schumann (ed.), *Atmospheric Physics*, Research Topics in Aerospace,
DOI: 10.1007/978-3-642-30183-4_27,

Lidar (Light detection and ranging) is certainly the best suited experimental setup for achieving this goal. It has been used in atmospheric physics for more than 40 years, and aerosol *remote sensing* is one of the main applications. The main reasons are that the *optical depth* of aerosols is normally low enough to prohibit complete attenuation of the emitted radiation, and that lidar can provide data during daytime and nighttime.

For radiative studies in general three categories of parameters are used to characterize atmospheric aerosols: spatial distribution, and the optical and microphysical properties of the particles. The first category concerns the most basic set of information, i.e., the vertical aerosol distribution and the extent of elevated layers as a function of time. The second category includes extinction and *scattering coefficients* and information on the angular distribution of scattering (*phase function*, asymmetry parameter). For deeper understanding of the interaction of particles with radiation, microphysical properties such as particle size, shape, mass concentration and *refractive index* are useful. Several (but not all) of these parameters can be derived from lidar measurements. The achievable accuracy and resolution depend on the physical concept of the measurement: a distinction is made between "*backscatter lidars*," "*Raman lidars*" and "*high spectral resolution lidars*" (HSRL). *Polarimetric* measurements can be considered as an add-on. "*Differential absorption lidars*" are not considered, although in principle they can be used for aerosol remote sensing in the same way as backscatter lidars.

The main part of the paper will focus on different aerosol products that can be derived by lidar, starting with a brief introduction to the basics of lidar methodology and closing with a short overview of recent lidar applications.

27.2 Lidar Concept

The physical concept underlying a backscatter lidar is the emission of short *laser* pulses (at wavelength λ_0)—thus, it is called "active" remote sensing—and the time resolved detection of photons (of the same wavelength) backscattered from air molecules and particles (aerosols and clouds). Using the velocity of light, the time domain is transformed into the spatial domain. The spatial resolution is described as "range-bin" Δz. As the received signal depends on the amount and properties of the aerosols along the line of sight, lidar can in principle be used to characterize aerosol distribution.

The number of received photons from a range-bin at range z depends on the characteristics of the lidar system, e.g., the number of photons emitted per pulse and the length of the sampling interval, described by the lidar constant C_L. Furthermore, it depends on atmospheric conditions, i.e., on the efficiency of the backscattering of particles and air molecules at range z, and on the probability that emitted photons reach z and again the lidar after being backscattered, without being absorbed or scattered in arbitrary directions in between. Accordingly, one frequently used formulation of the basic equation of lidar remote sensing for a

monostatic (i.e., emitter and receiver are at the "same" place) backscatter lidar is given in Eq. 27.1. Note that the nomenclature in the literature is not standardized, and "the signal" may be expressed, e.g., in terms of number of photons, photoelectrons or power.

$$P(z,\lambda_0) = C_L \frac{\beta_m(z,\lambda_0) + \beta_p(z,\lambda_0)}{z^2} \exp\left\{ -2 \int_0^z [\alpha_m(z',\lambda_0) + \alpha_p(z',\lambda_0)]\, dz' \right\} \tag{27.1}$$

Here, $P(z,\lambda_0)$ is the number of backscattered photons from a range-bin at range z at wavelength λ_0, and C_L the above mentioned instrument constant. Backscatter and *extinction coefficients* are denoted as β (typically given in km^{-1} sr^{-1}) and α (typically in km^{-1}), respectively; subscripts p and m are added to distinguish between the contributions of particles and molecules. The exponential term is the two-way transmission of the atmosphere between the lidar and range z describing the above mentioned probabilities. Eq. 27.1 implicitly means that all photons that contribute to the signal, do not experience any further scattering between the lidar and z. Therefore, this equation is also referred to as the lidar equation in single scattering approximation. Numerical simulations have shown that multiple scattering can indeed be neglected in case of aerosol observations from ground, however, in cases of *satellite observations* multiple scattering can contribute to the signal.

Most aerosol lidars apply Nd:YAG lasers with a fundamental wavelength of 1 064 nm. Using frequency doubling and tripling crystals, simultaneous emission at 532 and 355 nm can be obtained. The specifications of the receiver are often quite different as they are optimized for specific scientific applications and measurement conditions; note that many lidars are research oriented. The receiver field of view is typically 1 mrad (FWHM) and slightly larger than the beam divergence of the laser. The pulse repetition frequency is in the order of 10–100 Hz, the spatial resolution in the order of a few meters to a few tens of meters.

As already mentioned, measurements of tropospheric aerosols are among the main scientific objectives of lidar. For this purpose, measurements should cover the range from the surface to the tropopause, or to the stratosphere if volcanic aerosols are to be observed. The lower limit should be as close as possible to the surface to minimize the loss of information in altitudes where the aerosol concentration is maximum. The near end of the range is primarily determined by the overlapping of the receiver field of view and the divergence of the emitted beam. Typically, full overlap is realized after several hundred meters up to more than one kilometer. As a consequence, significant parts of the *boundary layer* aerosol are "invisible" for a lidar. To overcome this drawback there are several options: measurements under different zenith angles can be combined, an optical design with an adjustable field of view can be implemented, or two or more receiving telescopes with different fields of view can be used.

The far end of the measurement range is important even for boundary layer observations because the upper aerosol-free troposphere is used for calibrating the lidar signals (the so called "Rayleigh calibration" or "Rayleigh fit"). Rayleigh calibration is required because C_L is not known with sufficient accuracy.

27.3 Retrieval of Geometrical Properties

Monitoring the spatial and temporal distribution of aerosols is comparably easy. This becomes obvious after introduction of the transmission T (and the optical depth τ of the atmosphere)

$$T(z,\lambda_0) = e^{-\tau(z,\lambda_0)} = \exp\left\{-\int_0^z \alpha(z',\lambda_0)\, dz'\right\} \quad \text{with} \quad \alpha = \alpha_p + \alpha_m$$

The exponential term in Eq. (27.1) can then be expressed as the two-way transmission $T^2(z)$ and the range corrected signal $P(z)z^2$

$$P(z)z^2 \propto \beta^* = \beta(z)\; T^2(z) \tag{27.2}$$

is accordingly proportional to the attenuated backscatter β^*.

For the interpretation of Eq. 27.2 it is useful to discuss the transmission: $T^2(z)$ only slowly decreases with range z starting from $T^2(0) = 1$. Keeping in mind that optical depth typically decreases with wavelength, the decrease of $T^2(z)$ is the smaller the larger the wavelength is. For example, for $\lambda_0 = 1\,064$ nm and under typical atmospheric conditions, the two-way transmission remains larger than approximately 0.9, and β^* is a good approximation for β. According to the Angström approach

$$\alpha_p \propto \lambda^{-\kappa} \quad \text{and} \quad \alpha_m \propto \lambda^{-4.08} \tag{27.3}$$

with typically $\kappa < 2$ it becomes obvious that the influence of air molecules compared to aerosols is drastically reduced at long wavelengths. As a consequence, $\beta = \beta_m + \beta_p$ is dominated by β_p so that any spatial discontinuity in the aerosol distribution is clearly visible in β^*. Note that β_m is a smooth function with height.

As a result, the stratification of aerosols, e.g., the top of the *planetary boundary layer* or the residual layer, and the height and vertical extent of elevated layers, can easily be monitored from range corrected signals. Most state-of-the-art backscatter lidars include a detection channel at 1 064 nm so that a temporal resolution of a few minutes can be achieved; shorter wavelengths are less suitable but sufficient for most applications. An example is given in Fig. 27.1. Shown is the range corrected signal (arbitrary units, color coded) at 1 064 nm as derived at Maisach (25 km northwest of Munich) from the three-wavelength Raman *depolarization*

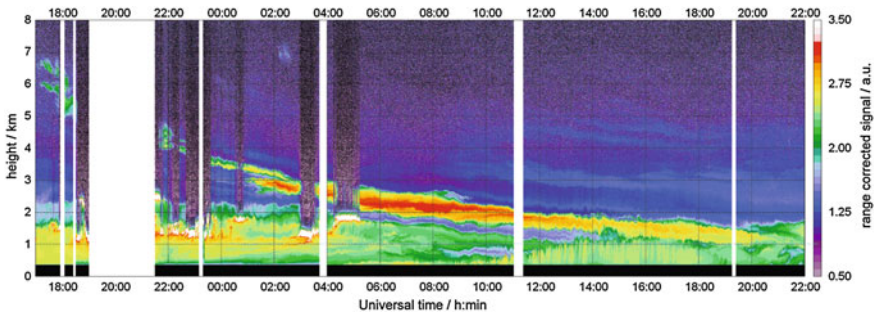

Fig. 27.1 Range corrected signal (log. scale, a.u.) at 1 064 nm versus height above mean sea level as derived from MULIS:, 17:00 UTC 16 April 2010 until, 22:00 UTC 17 April 2010, at Maisach (25 km northwest of Munich) showing the advent of the ash layer (see text) from the Eyjafjallajökull eruption. MULIS is the three-wavelength Raman depolarization lidar of MIM. The lowermost 350 m are influenced by the incomplete overlap (shown in *black*)

lidar MULIS of the Meteorological Institute at Munich (MIM) two days after the *eruption* of the Icelandic *volcano Eyjafjallajökull* (Wiegner et al. 2011). The aerosol stratification is immediately clear without any complex numerical *inversion* scheme: a pronounced layer appeared at about 7 km at 17:00 UTC 16 April 2010, and descended to about 4 km at midnight. The layer further descended but was still separated from the residual layer until the afternoon of 17 April. After 17:00 UTC mixing with the boundary layer took place. Figure 27.1 also shows faint aerosol structures throughout the free troposphere from 09:00 UTC 17 April. It should be emphasized that it is intuitively clear that the pronounced layer was the *ash* plume of the volcanic eruption, but from the range corrected signal alone there is no strict evidence.

The fact that backscattering at $\lambda_0 \approx 1\,\mu m$ is very well suited for monitoring aerosol distribution and transport led to an increasing awareness of lidar technology for the surveillance of atmospheric aerosols. It gave rise to the implementation of ceilometer networks; the German Weather Service recently set up a network of almost sixty *ceilometers* in Germany. Ceilometers are single-wavelength backscatter lidars with quite low laser pulse energies but higher pulse repetition rate. They are eye-safe and can thus be operated unattended and continuously. They are going to be used to monitor the temporal development of the boundary layer and the dispersion of aerosol plumes.

27.4 Retrieval of Optical Properties

For radiative studies the provision of range corrected signals (previous section) is not sufficient; quantitative evaluation of optical properties is conclusive. From Eq. (27.1) it is clear that the aerosol related *optical property* is either α_p or β_p. Equation (27.1) however includes four unknown meteorological variables—α_m,

β_m, α_p, and β_p. Thus, it is obvious that the quantity of interest cannot be retrieved without further information.

From Rayleigh theory it is known, that the optical properties of air molecules, $\alpha_m(z,\lambda)$ and $\beta_m(z,\lambda)$, can be calculated with high accuracy from air density profiles. Air density is determined according to the ideal gas law using profiles of pressure and temperature from *radiosonde* ascents. Therefore, they are considered as known in the lidar equation. Nevertheless, the lidar equation is underdetermined as two unknowns remain: α_p and β_p. This problem is formally solved by introducing a relationship between α_p and β_p, the so called *lidar ratio* S_p.

$$S_p(\lambda) = \frac{\alpha_p(\lambda)}{\beta_p(\lambda)} \tag{27.4}$$

Thus, the main problem of the inversion of the lidar equation is the need to find the correct lidar ratio; note that S_p depends on the aerosol type (see below).

27.4.1 Backscatter Lidar

A backscatter lidar is the least complicated and therefore by far the most frequently used configuration. It is based on elastic scattering under 180 degrees. The signals are described by the lidar Eq. (27.1) that can be solved analytically by the so called "*Klett method*" (Klett 1981; Fernald 1984). For α_p the solution reads (omitting λ_0 for simplicity):

$$\alpha_p(z) = \frac{Z(z)}{N(z)} - \frac{S_p(z)}{S_m} \cdot \alpha_m(z) \tag{27.5}$$

with

$$Z(z) = S_p(z) \cdot z^2 \cdot P(z) \cdot \exp\left\{ 2 \int_z^{z_{\mathrm{ref}}} \left[\frac{S_p(z')}{S_m} - 1 \right] \alpha_m(z') dz' \right\} \tag{27.6}$$

and

$$N(z) = \frac{S_p(z_{\mathrm{ref}})\ z_{\mathrm{ref}}^2\ P(z_{\mathrm{ref}})}{[S_p(z_{\mathrm{ref}})/S_m]\ \alpha_m(z_{\mathrm{ref}}) + \alpha_p(z_{\mathrm{ref}})} + 2 \int_z^{z_{\mathrm{ref}}} Z(z') dz' \tag{27.7}$$

It should be emphasized that analogously to Eq. 27.5 a solution for $\beta_p(z)$ can be found.

The solution for α_p requires a boundary value $\alpha_p(z_{\mathrm{ref}})$ at a reference height z_{ref}, as can be seen in Eq. 27.7 and the lidar ratio S_p (Eqs. 27.6 and 27.7). The reference

height is typically set to an altitude in the upper free troposphere where no aerosols are present. The reference height is found by comparing the measured signal and a modeled signal according to the Rayleigh atmosphere.

The lidar ratio of the air molecules S_m is known from Rayleigh theory and in good approximation wavelength-independent

$$S_m = \frac{8\pi}{3}\left(1 + \frac{\rho^n(\lambda)}{2}\right) \quad \text{with} \quad \rho^n = \begin{cases} 0.03016 & \text{at} \quad \lambda = 355\,\text{nm} \\ 0.02837 & \text{at} \quad \lambda = 532\,\text{nm} \\ 0.02719 & \text{at} \quad \lambda = 1064\,\text{nm} \end{cases}$$

To elucidate the complexity of S_p of the particles it is convenient to express it in terms of well-known parameters, the phase function p (normalized to 1) and the *single scattering albedo* ω_0 (ratio of scattering and extinction coefficient). Then

$$S_p(\lambda) = \frac{1}{\omega_0(\lambda) p(180^\circ, \lambda)} \tag{27.8}$$

As ω_0 and p depend on the refractive index m of the particles and their *size distribution* $n(r)$, it follows from Eq. 27.8 that S_p also depends on m and the particle size. Furthermore, the *microphysics* can change with height and *relative humidity*, thus, the same is true for S_p. However, most of this information is not available under normal conditions. As a consequence, the exact values of S_p along the lidar's line of sight are never known and one has to rely on plausible estimates. These can be based on model calculations or independent measurements.

In case of model calculations, the refractive index m and the radius r of the particle are required as input. For spherical particles the *Mie theory* is applied, but in cases of *nonspherical* particles more complex scattering models must be used and adequate parameters for the description of the shape must be defined. Depending on the shape and the size of the particle different approaches are available, e.g., the T-matrix method, discrete dipole approximation, the finite difference time domain method, or the geometrical optics approach. As already mentioned the microphysical properties and the meteorological conditions are unknown under normal conditions. Moreover, most of these models are computationally very expensive. As a consequence, the calculation of lidar ratios (and other aerosol properties) focusses rather on basic research than on routine application.

The alternative approach to get S_p-estimates relies on independent measurements (see next section). It has been found that the assignment of a type (e.g., dust, marine, biomass burning) to the aerosol (often referred to as "aerosol typing") is a feasible way to constrain the possible range of S_p. If the meteorological situation of the site and back trajectories are considered, aerosol typing is considered as sufficiently reliable. For wavelengths of 355 and 532 nm the lidar ratio typically is between 30 and 80 sr: for marine aerosols, lidar ratios are lower than 30 sr, for desert dust S_p is around 60 sr, and for biomass burning it is up to 80 sr. However, even if classification is possible, an uncertainty range of the order of ± 10 sr remains.

A consequence of the *uncertainty* of the lidar ratio estimate is uncertainty about the retrieved aerosol optical properties (α_p or β_p) in the order of up to 30 %. Therefore, α_p-profiles should always be treated with care and the assumption used for the S_p-estimate should be critically examined if backscatter lidars are deployed.

27.4.2 Raman Lidar

A *Raman lidar* (Ansmann et al. 1992) takes advantage of inelastic ("Raman") scattering of photons by molecules of known density, normally N_2. These photons are wavelength shifted and can be recorded separately from the elastically backscattered photons at the emitted wavelength. The wavelengths corresponding to emitted radiation at 532 and 355 nm are 607 and 387 nm, respectively. The height dependent Raman *backscatter coefficients* can be calculated from the known air density.

To exploit Raman lidar data, two equations are considered. The well-known equation for elastic backscattering at λ_0, Eq. 27.1, and a second equation for the corresponding Raman wavelength λ_R:

$$P(z,\lambda_R) = C_R \frac{\beta_R(z,\lambda_0)}{z^2} \exp\left\{ -\int_0^z \left[\alpha_p(z',\lambda_0) + \alpha_m(z',\lambda_0) + \alpha_p(z',\lambda_R) + \alpha_m(z',\lambda_R)\right] dz' \right\} \tag{27.9}$$

with β_R as the Raman backscatter coefficient. Equation 27.9 describes the signal at the Raman-shifted wavelength λ_R, which is governed by the transmission at λ_0 along the path from the lidar to the location of the scattering process and by the transmission at λ_R on the way back to the receiver. Equations 27.1 and 27.9 can be solved for the two unknowns $\alpha_p(\lambda_0)$ and $\beta_p(\lambda_0)$.

If more than one wavelength can be exploited, the wavelength-dependence of α_p can be used as a measure for the particle size. For this purpose the *Angström* exponent κ (see Eq. 27.3) is determined. As a rule of thumb, $0<\kappa<0.5$ indicates large particles (dust, humidified particles), whereas $1<\kappa<2$ is typical for small particles.

As the Raman lidar technique allows determination of α_p and β_p independently, it is possible to retrieve the lidar ratio. This is a fundamental difference to a backscatter lidar. Thus, Raman lidars are used to establish S_p-climatologies of different aerosol types, e.g., in the framework of the European aerosol research lidar network (EARLINET, see Bösenberg et al. 2003) and such dedicated *field campaigns* as the Saharan mineral dust experiment (SAMUM). These data sets can serve as estimate of the lidar ratio required for the Klett method.

As a consequence of the very low Raman backscatter coefficients, Raman lidars require powerful lasers, long averaging times of up to one or two hours, and very effective suppression of the solar background radiation. Therefore, most systems are restricted to nighttime operation only, and the temporal and spatial resolution of the retrieved aerosol profiles is limited. Technical solutions to provide daytime operation are underway.

27.4.3 Polarization Lidar

The previous sections have shown that the classification of aerosols ("aerosol typing") is a promising approach to find estimates of lidar ratios. Polarimetric measurements might also support aerosol typing. As it is known from electrodynamics that spherical particles do not change their original state of polarization, whereas nonspherical particles do, it is useful to implement two polarimetric channels to the lidar: one is oriented in the same plane as the emitted linear polarized radiation, the second perpendicular to it. Thus, polarimetric information can be used to distinguish between these two classes of particles.

For the sake of simplicity we do not want to consider cross-talk between the two channels. Then, the lidar Eq. (27.1) can be written separately for the co-polar channel

$$P_{\parallel}(z) = C_{\parallel}\beta_{\parallel}(z)\frac{1}{z^2}\exp\left\{-2\int_0^z \alpha(z')dz'\right\} \tag{27.10}$$

and the cross-polar channel

$$P_{\perp}(z) = C_{\perp}\beta_{\perp}(z)\frac{1}{z^2}\exp\left\{-2\int_0^z \alpha(z')dz'\right\} \tag{27.11}$$

In literature, sometimes $\beta_{\parallel}$ and $\beta_{\perp}$ are replaced by $(1 - d/2)\ \beta(z)$ and $(d/2)\beta(z)$, respectively. The depolarization parameter d can be calculated from scattering theory.

A convenient measure of the polarization state is the so-called volume linear depolarization ratio δ_v.

$$\delta_v = \frac{\beta_{\perp}}{\beta_{\parallel}} = \frac{d/2}{1-(d/2)} = \frac{C_{\parallel}}{C_{\perp}}\frac{P_{\perp}}{P_{\parallel}} = C_{\delta}\frac{P_{\perp}}{P_{\parallel}} \tag{27.12}$$

It can directly be derived as the ratio of the two lidar measurements provided that the calibration constant C_{δ} has been determined (Freudenthaler et al. 2009). No further information, in particular no lidar ratio, is required. However, δ_v is not an aerosol property as it depends on the relative contributions of aerosols and air molecules. Nevertheless, it can provide a first indication of the aerosol type, in

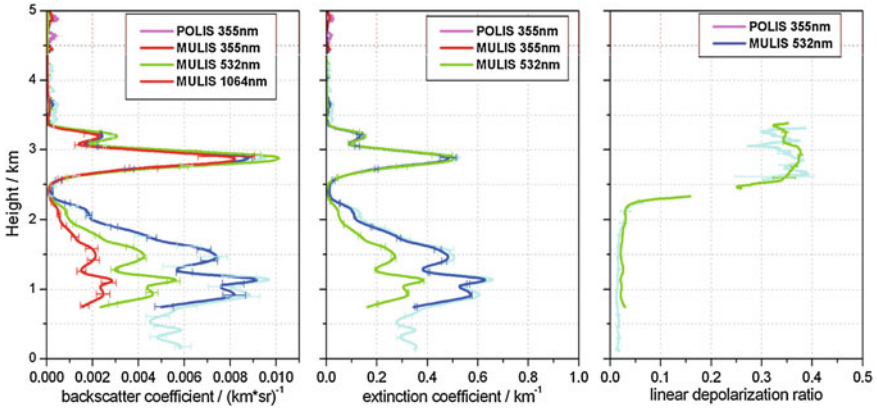

Fig. 27.2 Profiles of particle optical properties: backscatter coefficient, extinction coefficient and linear depolarization ratio as a function of height above ground; derived from MULIS and POLIS measurements at Maisach on 17 April 2010 between 01:30 and 02:40 UTC. The error bars indicate systematic errors (modified after Groß et al. 2011)

particular in cases where aerosols are the dominating component (e.g., in Saharan dust layers). A more accurate parameter describing aerosol properties is the particle linear depolarization ratio δ_p. It can be determined according to

$$\delta_p = (\delta_v + 1)\left(\frac{\beta_m(\delta_m - \delta_v)}{\beta_p(1 + \delta_m)} + 1\right)^{-1} - 1 \qquad (27.13)$$

The derivation of δ_p is more demanding: it requires knowledge of δ_v and β_p at the corresponding wavelengths, the latter normally retrieved from the Klett method with an estimated lidar ratio. δ_m is the depolarization ratio of air molecules and—again—known from Rayleigh theory; it is between 0.0036 and 0.0146 depending on the filter bandwidth of the detection channel. Typical values of δ_p for desert dust are between $0.25 < \delta_p < 0.35$ for wavelengths at 355 and 532 nm. Measurements over Munich during the *Eyjafjallajökull* eruption showed that for volcanic ash layers the values were even larger at $0.35 < \delta_p < 0.40$. Any other aerosol type shows significantly lower depolarization ratios. Though the data base of high quality depolarization measurements is still limited it is generally accepted that δ_p has a large potential for aerosol typing, and thus can help in better estimating lidar ratios for the Klett method. Furthermore, it was found that under certain conditions it is possible to estimate the mixing state of aerosols from δ_p-retrievals.

27.4.4 Optical Characterization of Aerosols

As an example of the potential of different lidar configurations, the characterization of the Eyjafjallajökull plume over Maisach (cf. Fig. 27.1) is again discussed.

With advanced lidar systems, i.e., systems including elastic backscatter detection, polarimetric measurements, and Raman channels at different wavelengths, a large set of optical properties of aerosols as shown in Fig. 27.2 can be retrieved. Here, results from the two MIM lidars, MULIS and POLIS (portable two-channel lidar), are combined, primarily to get depolarization ratios at two wavelengths.

Shown are profiles of β_p, α_p, and δ_p (from left to right) at three and two wavelengths, respectively. The β_p- and α_p-profiles are derived from the Klett method applying lidar ratios from the Raman method. It can be seen that β_p and α_p of the elevated layer are virtually wavelength-independent, whereas a significant decrease with wavelength occurs below 2 km. This is a clear indication that the particles of the lower layer are much smaller than in the upper layer, where the *Angström* exponent κ is close to zero. The profile of δ_p also reveals a significant difference between the elevated layer and lower altitudes. The large depolarization ratio suggests nonspherical particles. Both findings with respect to the size and shape of the particles clearly suggest that the elevated layer was indeed the ash plume of the volcano.

In case only a three-wavelength backscatter lidar is available, the characterization of the aerosols is limited to the β_p-profiles (left panel). As a consequence the vertical extent of the layer can be assessed, and from the wavelength dependence of β_p a rough estimate of the size of the particles. Note, that the Angström exponent is *per definitionem* related to α_p. However, as long as the lidar ratio does not change much with the wavelength, the wavelength-dependence of β_p can be used as an approximation. In case only a single-wavelength system is available (simple backscatter lidar, *ceilometer*) only the vertical extent of the layer can be found.

27.5 Retrieval of Microphysical Parameters

In the previous sections it was briefly demonstrated that optical properties can be used to estimate microphysical properties: the wavelength-dependence of α_p, expressed in terms of κ, is an indication of particle size, δ_p an indication of particle shape. Recently, measurements of optical properties, i.e., α_p and β_p at several wavelengths, were also used to retrieve the microphysical properties of the particles in a more rigorous way. Of special interest are the volume distribution $v(r)$ and the refractive index m, the latter primarily to estimate the single scattering albedo of atmospheric aerosols. A further quantity, the mass concentration M, came into focus during the *Eyjafjallajökull* eruption as this parameter is of highest relevance for *air traffic* safety.

The link between optical and microphysical properties is given by scattering theory according to

$$\alpha_p(\lambda) = \int_0^\infty Q_\alpha(r, \lambda, m) \frac{3}{4r} v(r) dr \tag{27.14}$$

$$\beta_p(\lambda) = \int_0^\infty Q_\beta(r, \lambda, m) \frac{3}{4r} v(r) dr \tag{27.15}$$

Q_α and Q_β are the extinction and backscatter efficiencies at wavelength λ for particles with a complex refractive index m and size r. In the case of spherical particles these functions are calculated from *Mie theory*, in the case of *nonspherical* particles more complex scattering models must be used (cf. Sect. 27.4.1). In the case of M, the density of the particles is required as an additional parameter. The inversion is an ill-posed problem, and thus the numerical implementation is critical. Further complications arise from the limited number of measured optical parameters (i.e., the left side of the equations) and the magnitude of the measurement errors.

As already mentioned, state-of-the-art multiwavelength Raman lidar measurements provide α_p at two wavelengths (355, 532 nm) and β_p at three wavelengths (355, 532, 1 064 nm). Measurements of these five optical properties are the minimum requirement for the inversion of Eqs. (27.14) and (27.15) for the volume distribution and the refractive index (Müller et al. 2001). Several case studies on the basis of Mie theory have shown that the inversion in principle is feasible, nevertheless, the accuracy of the retrieved parameters is often insufficient. Thus, the establishment of robust inversion schemes is a current research topic. Among others, more efficient numerical solutions are tested, the additional consideration of depolarization ratios is investigated, implying the application of scattering models for nonspherical particles and the combination of lidar and *sun- and sky-radiometers* data. The latter provide multiwavelength direct and diffuse radiances; however, in contrast to the lidar data, this information is "vertically integrated." This combined approach was applied to the retrieval of M in the case of the *Eyjafjallajökull* plume when Gasteiger et al. (2011) retrieved conversion factors from α_p to M. They demonstrated that the conversion factors critically depend on the size distribution of the particles and their shape. As a result the mass concentration can be retrieved with an uncertainty range of approximately ± 50 %.

27.6 Examples of Applications

As already mentioned, long term observations of aerosol distributions ("climatologies") as well as process studies to understand interactions between aerosols, clouds and radiation are required to improve knowledge of the *climate system*. Both issues can be supported by lidar. A few examples of current applications are briefly discussed below.

27.6.1 Closure Studies

Closure experiments are important, e.g., for understanding the interaction between radiation and aerosol particles, and they are the basis for testing and validating new

remote sensing schemes. To obtain a complete set of information, the vertical distribution of aerosol optical properties must be measured. Key contributions come from airborne *in-situ measurements* and lidars—deployed from ground and aircraft. This approach was realized in a series of aerosol characterization experiments, e.g., ACE-1, which was devoted to the pristine marine atmosphere, ACE-2, where anthropogenic aerosols from Europe and transported desert dust were investigated, ACE-Asia which focused on anthropogenic aerosols over the Asian Pacific region, and most recently SAMUM, which concentrated on mineral dust aerosols.

In the framework of SAMUM, three ground-based *Raman lidar* systems (of MIM and IfT, Leipzig) and the airborne high spectral resolution lidar of DLR were operated. The scientific goal of the measurements included several of the topics mentioned in the previous sections: assessment of the lidar ratio of Saharan dust and the changes due to aging, investigation of the spectral dependence of the depolarization ratios, *validation* of scattering models for nonspherical particles, and development of strategies to characterize aerosol mixtures by means of lidar measurements.

27.6.2 Networks

To get long term observations for the assessment of the variability and trends, lidar networks can provide substantial contributions. As advanced lidar systems are a quite expensive technology, the number of stations and the temporal sampling will always be limited and the representativeness might suffer. Thus, recent activities to establish lidar networks focus rather on research (improvement of data evaluation, development of synergistic methodologies, standardization of hardware, automatization) than on monitoring.

The first ground-based lidar network following this concept was established in Germany in 1997 with five stations, including MIM. This small network was working on a regular basis, had agreed on common data products and formats, and had for the first time undergone strict quality assurance on hardware and software level. In 2000 the network was extended to the "European Aerosol Research Lidar Network" (EARLINET) and now includes 27 stations.

During the last few years other networks were established outside Europe, e.g., the "Asian Dust Network," "REALM" (Eastern United States), the "CIS-LiNet" (former Soviet Union) and "ALINE" (South America). The objectives, the degree of cooperation and maturity, and strategies for data exchange are not yet harmonized; however, the *World Meteorological Organization* initiated first steps to combine the different continental networks under the umbrella of "GALION" (GAW Aerosol Lidar Observation Network). However, in view of monitoring, networks of "low cost" standardized systems that can be operated unattended and continuously must be implemented. Concepts for the combination of a limited number of high-end systems and a denser network of ceilometer-type instruments are currently under investigation.

The lidar networks mentioned above have been active for about one decade, and primarily concentrate on tropospheric aerosols. In the case of stratospheric aerosols, long-term observations are already available. Due to the long residence time and the larger spatial homogeneity of stratospheric aerosols, the requirements with respect to the number of stations and the temporal sampling are relaxed. The most consistent time series is available for Garmisch-Partenkirchen (Germany) and covers 30 years (Jäger 2005). It documents a close correlation between stratospheric aerosol load and volcanic eruptions.

27.6.3 Lidar in Space

Though ground-based networks have proved to be of great benefit for characterizing aerosols on larger scales, spaceborne observations are indispensable to ultimately provide global aerosol data sets. The first spaceborne lidar experiment was the Space Shuttle mission LITE, (Lidar in Space Technology Experiment) conducted by NASA in September 1994. LITE had a three-wavelengths *backscatter lidar* on board with the inherent difficulties in deriving quantitative aerosol parameters (see Sect. 27.4.1), but it successfully demonstrated the feasibility of active aerosol monitoring from space.

The first long term mission is *CALIPSO* (Cloud-Aerosol Lidar and Infrared Pathfinder Satellite Observations Experiment) launched in April 2006 and still in operation. Again, a backscatter lidar is used, including polarimetric measurements at 532 nm. To take advantage of complementary measurements CALIPSO is flown as a part of a multisatellite constellation (A-train). In parallel to the spaceborne measurements, extensive ground truth campaigns are conducted to verify the aerosol retrievals. In particular, the accuracy of the assumed lidar ratios is critically reviewed.

The first European long-term spaceborne mission including an aerosol lidar will be *EarthCARE* (Earth Clouds, Aerosols and Radiation Explorer). It is planned to implement a high spectral resolution lidar. As a consequence, no estimates of lidar ratios will be required. The tentative launch year is 2015.

27.7 Summary

The development of lidars for atmospheric research in the 1970s constituted a new era of aerosol remote sensing by providing range resolved information. At that time, however, aerosol distributions could only be determined qualitatively. Only the advent of powerful lasers and improved detection systems in the 1990s allowed the quantitative derivation of aerosol optical properties. After the turn of the century it was demonstrated that under favorable conditions even microphysical properties can be inferred from advanced lidar systems.

Applications of lidars in atmospheric science are numerous: From the beginning lidar measurements were mostly applied in dedicated field campaigns and aircraft missions (e.g., Mörl et al. 1981). Such studies were primarily set up to improve

and validate aerosol retrievals (e.g., from space), to understand the *radiative forcing* of aerosols and interactions with clouds. To increase the representativeness of aerosol profiling and to investigate spatial and temporal long term trends, lidar networks were established in the last decade. The most prominent example is EARLINET, a European network consisting of more than twenty sites with state-of-the-art lidar systems. To what extent secondary networks of *ceilometers* as currently being implemented by national weather services can improve knowledge of the four-dimensional distribution of aerosols is presently under discussion. There is a strong demand for such data for *numerical weather prediction* and in contingency cases, e.g., volcanic eruptions. In this context the provision of aerosol profiles in near-real-time is of special importance.

In parallel to the growing number of ground-based lidar systems, spaceborne missions were defined to provide global coverage. *CALIPSO*, with a dual-wavelength backscatter lidar, was launched in 2006 providing new perspectives in aerosol remote sensing, in particular when different satellite sensors are ultimately exploited synergistically.

In the next few years, efforts must be intensified to make use of lidar data for numerical weather prediction and climate modeling, and to exploit synergies between lidar, radar and passive remote sensing. With respect to aerosols, investigations of their indirect effects, in particular, will move into the focus of attention.

References

Ansmann, A., Wandinger, U., Riebesell, M., Weitkamp, C., Michaelis, W.: Independent measurement of extinction and backscatter profiles in cirrus clouds by using a combined raman elastic-backscatter lidar. Appl. Opt. **31**(33), 7113–7131 (1992)

Bösenberg, J., V. Matthias, A., Amodeo, V., Amoiridis, A., Ansmann, J., Baldasano, M., Balin, I., Balis, D., Böckmann, C., Boselli, A., Carlsson, G., Chaikovsky, A., Chourdakis, G., Comeron, A., De Tomasi, F., Eixmann, R., Freudenthaler, V., Giehl, H., Grigorov, I., Hagard, A., Iarlori, M., Kirsche, A., Kolarov, G., Komguem, L., Kreipl, S., Kumpf, W., Larcheveque, G., Linné, H., Matthey, R., Mattis, I., Mekler, A., Mironova, I., Mitev, V., Mona, L., Müller, D., Music, S., Nickovic, S., Pandolfi, M., Papayannis, A., Pappalardo, G., Pelon, J., Perez, C., Perrone, R.M., Persson, R., Resendes, D.P., Rizi, V., Rocadenbosch, F., Rodrigues, J.A., Sauvage, L., Schneidenbach, L., Schumacher, R., Shcherbakov, V., Simeonov, V., Sobolewski, P., Spinelli, N., Stachlewska, I., Stoyanov, D., Trickl, T., Tsaknakis, G., Vaughan, G., Wandinger, U., Wang, X., Wiegner, M., Zavrtanik, M., Zerefos, C.: EARLINET: A European Aerosol Research Lidar Network to Establish an Aerosol Climatology. MPI-Report 348, Max-Planck-Institut für Meteorologie, Hamburg, Germany, p. 192, ISSN 0937-1060 (2003)

Fernald, F.G.: Analysis of atmospheric lidar observations: some comments. Appl. Opt. **23**(5), 652–653 (1984)

Freudenthaler, V., Esselborn, M., Wiegner, M., Heese, B., Tesche, M., Ansmann, A., Müller, D., Althausen, D., Wirth, M., Fix, A., Ehret, G., Knippertz, P., Toledano, C., Gasteiger, J., Garhammer, M., Seefeldner, M.: Depolarization-ratio profiling at several wavelengths in pure Saharan dust during SAMUM 2006. Tellus B **61**, 165–179 (2009). doi:10.1111/j.1600-0889.2008.00396.x.

Gasteiger, J., Groß, S., Freudenthaler, V., Wiegner, M.: Volcanic ash from Iceland over Munich: mass concentration retrieved from ground-based remote sensing measurements. Atmos. Chem. Phys. **11**(5), 2209–2223 (2011). doi:10.5194/acp-11-2209-2011

Groß, S., Freudenthaler, V., Wiegner, M., Gasteiger, J., Geiß, A., Schnell, F.: Dual-wavelength linear depolarization ratio of volcanic aerosols: lidar measurements of the Eyjafjallajökull plume over Maisach, Germany. Atmos. Environ. **48**, 85–96 (2011). doi:10.1016/j.atmosenv.2011.06.017

Jäger, H.: Long-term record of lidar observations of the stratospheric aerosol layer at Garmisch-Partenkirchen. J. Geophys. Res. **110**, D08106 (2005). doi:10.1029/2004JD005506

Klett, J.D.: Stable analytical inversion solution for processing lidar returns. Appl. Opt. **20**, 211–220 (1981)

Mörl, P., Reinhardt, M.E., Renger, W., Schellhase, R.: The use of the airborne lidar ALEX-F for aerosol tracing in the lower troposphere. Contr. Atmos. Phys. **45**, 403–410 (1981)

Müller, D., Wandinger, U., Althausen, D., Fiebig, M.: Comprehensive particle characterization from three-wavelength Raman-lidar observations: case study. Appl. Opt. **40**(27), 4863–4869 (2001)

Wiegner, M., Gasteiger, J., Groß, S., Schnell, F., Freudenthaler, V., Forkel, R.: Characterization of the Eyjafjallajökull ash-plume: potential of lidar remote sensing. Phys. Chem. Earth (2011). doi:10.1016/j.pce.2011.01.006